# Photoluminescence of tetrahedrally coordinated $a$-$Si_{1-x}C_x$:H

Leandro R. Tessler* and Ionel Solomon
*Laboratoire de Physique de la Matière Condensée, Ecole Polytechnique, 91128 Palaiseau CEDEX, France*
(Received 12 December 1994; revised manuscript received 11 April 1995)

We have measured photoluminescence spectra of a series of hydrogenated amorphous silicon-carbon alloys $a$-$Si_{1-x}C_x$:H ($0<x<0.4$) prepared by plasma-enhanced chemical-vapor deposition from $SiH_4/CH_4$ mixtures. The power delivered to the plasma during the depositions was below the threshold of primary decomposition of $CH_4$ ("low power regime"). Carbon in the samples is mostly in the form of $-CH_3$ groups, keeping its $sp^3$ hybridization from the gas in the solid. These samples are tetrahedrally coordinated in the sense that they do not have $sp^2$ carbon. They have higher gap and are more strained than ordinary "high-power" alloys with corresponding carbon contents. The results indicate that for low carbon concentrations (including pure $a$-Si:H) the photoluminescence spectra are determined by static disorder only, electron-phonon effects being negligible. The effective disorder for radiative recombination is higher than the disorder probed by optical absorption. For higher carbon contents, high room-temperature luminescence efficiences (of the order of that of $a$-Si:H) with very small temperature dependence are found. This is interpreted as due to the enhancement of a fast excitonlike recombination process.

## I. INTRODUCTION

Amorphous hydrogenated silicon-carbon alloys ($a$-$Si_{1-x}C_x$:H) have been extensively studied in the past few years.[1] Alloying $a$-Si:H with carbon widens its gap and shifts the photoluminescence (PL) and electroluminescence spectra to higher energies. Presently, the main application of $a$-$Si_{1-x}C_x$:H is the $p$-type window layer in amorphous-silicon–based solar cells of improved efficiency,[2] which takes advantage of the gap widening. Visible light-emitting devices with $a$-$Si_{1-x}C_x$:H active layers operating at room temperature have already been obtained.[3] Like $a$-Si:H, $a$-$Si_{1-x}C_x$:H can be deposited by plasma-enhanced chemical-vapor deposition (PECVD) in large areas making electroluminescent flat panel displays an important potential application. The realization of this application depends on the comprehension and control of the PL mechanism in the material.

Pure $a$-Si:H of electronic quality (low density of states at the Fermi level) presents a featureless, slightly asymmetric, very intense $\sim$0.2-eV-wide PL band centered at $\sim$1.3–1.4 eV at low temperatures. The mechanism determining the PL band shape is still controversial.[4] The Stokes-shift model, proposed by Street,[5] attributes the PL band features to a strong electron-phonon coupling. The static disorder or zero-phonon model, developed by Dunstan and Boulitrop,[6] assigns the PL band shape to the distribution of carriers in both band tails that result from the disorder. Both mechanisms can in principle coexist and add to determine the PL band. Searle and Jackson[7] noted that the PL band width variation upon alloying could be used to elucidate the determinant process. They studied $a$-$SiN_x$:H alloys with different nitrogen contents and concluded that the static disorder model alone provides the best description of the PL over a wide composition range, including pure $a$-Si:H.

Being an element of the column IV of the periodic table, carbon could in principle incorporate substitutionally in the amorphous silicon network. However, the peculiar chemistry of carbon makes such incorporation very unlikely with the usual sample preparation process. At the temperature and pressure conditions used for sample preparation the $sp^2$ hybridization has a slightly lower configurational energy than the $sp^3$ hybridization. This is the opposite of silicon or germanium, for which the $sp^3$ hybrid is much more stable than the $sp^2$. Carbon atoms tend to form a mixture of diamondlike $\sigma$ bonds and graphitelike $\pi$-bonded clusters in $a$-$Si_{1-x}C_x$:H if the system is allowed to reach its lower-energy configuration. However, saturated $sp^3$ carbon hybrids as in $CH_4$ are very stable, due to high amount of energy necessary to break a C-H bond. Samples of $a$-$Si_{1-x}C_x$:H prepared by PECVD from $SiH_4/CH_4$ gas mixtures can have as precursors either saturated carbon (the low-power regime[8]) or unsaturated carbon (the high-power regime). These preparation conditions will be characterized in Sec. II A.

Several authors reported PL studies of $a$-$Si_{1-x}C_x$:H prepared under diverse high-power conditions. Sussmann and Ogden[9] studied PECVD samples prepared from $SiH_4/C_2H_2$ gas mixtures. They observed a single PL peak that widens and shifts to higher energies as the carbon content increases, and concluded that the zero phonon contribution to the PL is very important, and attributed the reduced temperature quenching in carbon-rich samples to a stronger Coulomb interaction between carriers. Siebert *et al.*[10] prepared samples from $SiH_4/CH_4$ mixtures, and reported a very strong decrease in the radiative lifetime $\tau_r$ for high carbon contents. These authors pointed out the correlation between PL peak position and width and the Urbach parameter. Liedtke *et al.*[11] proposed that for high carbon content the fast radiative recombination takes place in $sp^2$-

0163-1829/95/52(15)/10962(10)/$06.00  

bonded clusters. More recently, the St. Petersburg group[12,13] reported the coexistence of fast and slow radiative processes for samples with low carbon content, with only the fast component remaining in samples with high carbon contents and high luminescence efficiencies.

In the present paper we report a PL study in low-power $a$-$Si_{1-x}C_x$:H, an alloy that is structurally closer to $a$-Si:H than $a$-$SiN_x$:H or conventional high-power $a$-$Si_{1-x}C_x$:H, even though carbon is not substitutional in the sense of replacing silicon atoms at random. In low-power $a$-$Si_{1-x}C_x$:H carbon is incorporated onto the network primarily as methyl groups. We explored a wide range of energy gaps and Urbach parameters. For $x<0.2$ in fact virtually all carbon is in the form of methyl: the hydrogen concentration[8,14,15] $C_H$ varies as $3x$, the density of states (DOS) at the Fermi level[16] changes very little with $x$ and the "average gap" changes as the optical gap.[17] Van Swaaij *et al.*[14] have shown that as $x$ increases above $x=0.1$ the average number of hydrogen atoms bound to C decreases. They attributed this to surface reactions of the methyl groups. In our films, these reactions become important only for $x>0.2$, probably because of lower atomic bombardment during growth (see the last paragraph of Sec. II A). For $x>0.2$ the slope of $C_H$ is smaller than $3x$,[8,14] the DOS at the Fermi level increases very abruptly (faster than the density of paramagnetic centers[16]), and the slope of the "average gap" variation becomes higher. This indicates that for $x>0.2$ there is a change in the bonding of carbon. There are indirect indications of the formation of C-Si and C-C bonds.[8]

As far as the PL results are concerned, there are clearly two different recombination mechanisms, each dominating in a different carbon concentration range. For the low carbon content range ($x<0.2$) we confirmed the main conclusion of Searle and Jackson,[7] that only static disorder determines the PL band in the alloys and in pure $a$-Si:H as well. In contrast to $a$-$SiN_x$:H, for low-power $a$-$Si_{1-x}C_x$:H the static disorder model correctly predicts not only the dependence of the luminescence bandwidth on the disorder but also the shape of the low-energy branch of the PL band. We also show that the characteristic energy of the exponential density of states available for recombination is higher than the Urbach parameter related to subband gap light absorption.

For higher $x$ the PL intensity is narrower than expected from the static disorder model and depends very weakly on the temperature between 77 and 300 K. For $x=0.4$ the PL efficiency is only a factor 2 below that of pure $a$-Si:H at 77 K, although the density of states at midgap is much higher. This is interpreted as an indication that the radiative process becomes much faster as $x$ increases. The factors leading to this effect are discussed.

## II. EXPERIMENT

### A. Sample preparation

The preparation of $a$-$Si_{1-x}C_x$:H by PECVD is much more complicated than the preparation of pure $a$-Si:H. The simplest precursor gas mixture that can be used consists of $SiH_4$ and $CH_4$. That the dissociation energies of these two gases is not equal causes very different deposition conditions depending on the power delivered to the plasma in the reactor chamber. If the power delivered is high enough, both $SiH_4$ and $CH_4$ are decomposed primarily and the sample formation is dominated by the surface processes in the growing film. This is the high-power (HP) regime, in which most of the samples studied in the literature are prepared. If, however, the power delivered to the plasma is between the threshold of primary decomposition of $SiH_4$ and that of $CH_4$ all the carbon incorporated in the film results from secondary decomposition of $CH_4$ by the debris resulting from the primary decomposition of $SiH_4$. This characterizes the low-power (LP) regime,[8] in which methyl radicals ($CH_3$) are the only form of reactive carbon in the plasma during deposition. Since the carbon atoms remain saturated through the whole deposition process, $sp^3$ hybridization is maintained in the growing solid. In the low-power regime the incorporation of a carbon atom to the film involves a chemical reaction with at least one silicon radical, and this limits the carbon content of LP $a$-$Si_{1-x}C_x$:H to $x<0.5$. Indeed, the deposition rate tends to zero as the gas flow ratio $g=[CH_4]/([CH_4]+[SiH_4])$ tends to unity.[8,14,18] As long as there is enough $SiH_4$ to produce $CH_4$ decomposition, the carbon content depends very weakly on reactor parameters such as gas partial pressures and flow rates, substrate temperature, etc.

High-power $a$-$Si_{1-x}C_x$:H samples normally contain a mixture of $sp^3$ and $sp^2$ carbon hybrids. The $sp^2$ hybrid of carbon has a lower configuration energy than the $sp^3$ hybrid in the deposition conditions, so unsaturated carbon obtained from the primary decomposition of $CH_4$ may form $\pi$ bonds with a neighboring carbon in the solid. The presence of $\pi$ states affects in many aspects the electronic properties of the material. In contrast, the low-power deposition technique yields $a$-$Si_{1-x}C_x$:H with virtually no $sp^2$ carbon hybrids[8,17] up to $x\sim0.2$. We present evidence below that even above $x\sim0.2$ most of the carbon consists of $sp^3$ hybrids.

The samples studied were prepared by low-power PECVD decomposition of $SiH_4/CH_4$ mixtures, with $g$ between 0 and 0.995. In all depositions, the following parameters were kept constant: total pressure $\sim$40 mTorr, power density $\sim$0.06 W cm$^2$, total gas flow $\sim$4 l h$^{-1}$. Both glass (for the optical measurements) and roughened glass (for PL measurements) substrates were kept at 250°C during the deposition. Under these optimized conditions the deposition rate for pure $a$-Si:H was $\sim$0.8 $\mu$m h$^{-1}$, and did not depend on $g$ up to $g\sim0.85$, but started to decrease considerably above this value of $g$. Different carbon contents in the films were obtained by varying $g$. All samples are approximately 1 $\mu$m thick. The carbon content in the films was calculated fitting chemical reaction rate equations to the results of direct chemical analysis of 5 samples[8] and the extreme $x(g=0)=0$. Analytical chemistry methods require large amounts of material, being impractical for $x>0.3$ due to the reduced deposition rate. In the absence of a direct measurement, the carbon concentration is estimated from the extrapola-

tion of the fit for lower concentrations. We are aware of the uncertainty of this procedure, since this concentration range corresponds to a plasma regime where the reactions are modified by the lack of chemically active radicals ("starving regime"). Nevertheless, the value of $x$ is expected to continue growing with $g$ and not to exceed 0.5.

### B. Measurements

Optical transmission spectra for $0.01 < \alpha d < 5$ were measured by a conventional double beam spectrophotometer. The thickness $d$, the refractive index $n_0$, and the absorption coefficient $\alpha(h\nu)$ for each sample were calculated from these data.

Photoluminescence was measured at room temperature and at 77 K with the samples placed in a liquid-nitrogen cryostat. Excitation was provided by one of the unfocused lines of a $Kr^+$ laser. The excitation energies for each sample (between 1.6 and 3.5 eV) were as close as possible to $E_{04}$, the value of $h\nu$ for which $\alpha = 10^4$ cm$^{-1}$. The luminescence signal was filtered, dispersed by a 25-cm monochromator and detected by two-color (Si and thermoelectrically cooled InGaAs) photodiodes using standard in-phase techniques at 16 Hz. The spectral sensitivity of the whole system was calibrated by a tungsten halogen lamp.

All spectra were taken at laser intensities below $10^{18}$ photons cm$^{-2}$ sec$^{-1}$. We verified that in the measurement conditions the PL intensity depends linearly on the excitation intensity. All the discussion of PL results supposes germinate recombination.

## III. RESULTS AND DISCUSSION

### A. Optical absorption

For the $a$-$Si_{1-x}C_x$:H system, the commonly used Tauc extrapolation is not a reliable procedure to characterize the optical gap. In order to have reliable values for the optical gaps, the $(\alpha h\nu)^{1/2}$ vs $h\nu$ curve should be linear over at least one decade, a condition that is not verified in general for carbonated material in the range of $\alpha$ measured.[19] Instead we characterize our samples by $E_{04}$. This value is closer to the true mobility gap than the Tauc gap. Nevertheless, a Tauc plot for our pure $a$-Si:H sample yields a Tauc gap of 1.7 eV.

The exponential slope of the subgap absorption tail (the Urbach parameter $E_u$) was obtained from optical transmission down to $\alpha = 500$ cm$^{-1}$ and by photothermal deflection spectroscopy (PDS). The results from both techniques are in good agreement for $E_u$ above 0.150 eV. The values of the gas concentration ratio $g$, the carbon content $x$, the thickness $d$, the gap $E_{04}$, the Urbach parameter $E_u$, and the infrared refraction index $n_0$ for each sample are listed in Table I.

In a recent paper, Robertson[20] discussed the results of the virtual crystal approximation for $a$-$Si_{1-x}C_x$:H. Neglecting the effects of topological disorder, in a purely $\sigma$-bonded alloy (absence of $sp^2$ hybrids), any band energy $E_a$ is given by the linear combination

$$E_a = E_{Si}N_{Si\text{-}Si} + E_{SiC}N_{Si\text{-}C} + E_C N_{C\text{-}C} , \quad (1)$$

where $E_{Si}$, $E_{SiC}$, and $E_C$ are the energies of the respective band in crystalline silicon, SiC, and diamond, and $N_{Si\text{-}Si}$, $N_{Si\text{-}C}$, and $N_{C\text{-}C}$ are the concentration of the respective types of bonds in the alloy. For a random-bonding alloy,

$$N_{Si\text{-}Si} = (1-x)^2 , \quad N_{Si\text{-}C} = 2x(1-x) , \quad N_{C\text{-}C} = x^2 \quad (2)$$

and for a perfectly chemically ordered alloy with $x \leq 0.5$:

$$N_{Si\text{-}Si} = 1-2x , \quad N_{Si\text{-}C} = 2x , \quad N_{C\text{-}C} = 0 . \quad (3)$$

Low-power alloys present a special case of chemical order, in the sense that $x \leq 0.5$ and each carbon atom is bonded to one silicon. Then the bond concentrations are

$$N_{Si\text{-}Si} = 1-x , \quad N_{Si\text{-}C} = x , \quad N_{C\text{-}C} = 0 . \quad (4)$$

The gap is computed by the difference between the band edges, that are Si-like in this concentration range. The inclusion of hydrogen has the effect of widening the gap. The case of SiHCH bonding was calculated by Robertson. For low-power samples the correct form to obtain the effect of hydrogenation is to consider $SiHSiCH_3$. However, Eq. (3) can be viewed as a valid approximation, since the smaller gap increase predicted by Eq. (4) is compensated by the stronger gap widening

TABLE I. Carbon ratio $x$ = [C]/([C]+[Si]), thickness $d$, optical gap $E_{04}$, Urbach parameter $E_u$ and far-infrared refractive index $n_0$ as a function of the gas flow ratio $g$ = [$CH_4$]/([$CH_4$]+[$SiH_4$]).

| $g$ | $x$ | $d$ ($\mu$m) | $E_{04}$ (eV) | $E_u$ (eV) | $n_0$ |
|---|---|---|---|---|---|
| 0.00 | 0.00 | 0.93 | 1.93 | 0.060 | 3.32 |
| 0.50 | 0.07 | 1.14 | 2.01 | 0.070 | 3.02 |
| 0.60 | 0.10 | 1.08 | 2.22 | 0.091 | 2.72 |
| 0.80 | 0.19 | 0.92 | 2.52 | 0.161 | 2.18 |
| 0.87 | 0.24 | 1.06 | 2.66 | 0.180 | 2.07 |
| 0.92 | 0.29 | 0.94 | 2.71 | 0.215 | 1.89 |
| 0.95 | 0.33 | 0.85 | 3.29 | 0.265 | 1.84 |
| 0.975 | 0.37 | 0.95 | 3.44 | 0.295 | 1.80 |
| 0.98 | 0.38 | 0.96 | 3.56 | 0.362 | 1.78 |
| 0.99 | 0.40 | 1.29 | 3.36 | 0.350 | 1.76 |

effect of $CH_3$ respective to CH.

Figure 1 represents the gap $E_{04}$ versus carbon content obtained by different laboratories[9,10,14,18,21–26] as well as the results from Robertson's calculation.[20] Only samples prepared in the low-power regime[14,18,25] present the predicted values and linear dependence of the gap on the concentration over an extended range. We follow Roberston[20] and attribute the smaller gap systematically observed in HP samples to the presence of important amounts of $sp^2$ carbon hybrids. Note that our sample with the highest carbon content ($x=0.40$) has $E_{04}$ lower than the one with $x=0.38$. In fact for this sample the exponential absorption tail extends well above $E_{04}$. The absorption at $E_{04}$ is still dominated by the disorder, and in this case $E_{04}$ is not the good parameter to define the optical gap. It should always be remembered that the concept of a gap becomes ill defined when $E_u$ increases.

The formation of graphitic bonds relaxes the network by reducing the average atomic coordination and also because the $\pi$ bonds have one topological degree of freedom more than the $\sigma$ bonds. As a consequence, the potential fluctuations near the band edges are reduced and therefore a steeper Urbach tail is formed. In contrast, low-power samples are severely strained. A plot of the Urbach parameters $E_u$ as a function of carbon content (Fig. 2) displays this feature: the low-power samples have systematically higher $E_u$ than high-power samples with similar carbon content.

Another special characteristic of the samples studied is that they are prepared in a reactor with an extremely asymmetric electrode configuration (highly anodic deposition), in order to minimize atomic bombardment in the growing film. This guarantees that the methyl groups are left undisturbed after they are incorporated onto the film. This minimizes the formation of $sp^2$ carbon hybrids after deposition. Atomic bombardment during low-power growth may also promote network relaxation by assisting bonding between carbons already bonded to one silicon and a second silicon or a carbon neighbor. This is possibly why low-power samples prepared by different groups may present gaps lower than that predicted by Eq. (3) when the carbon concentration increases.

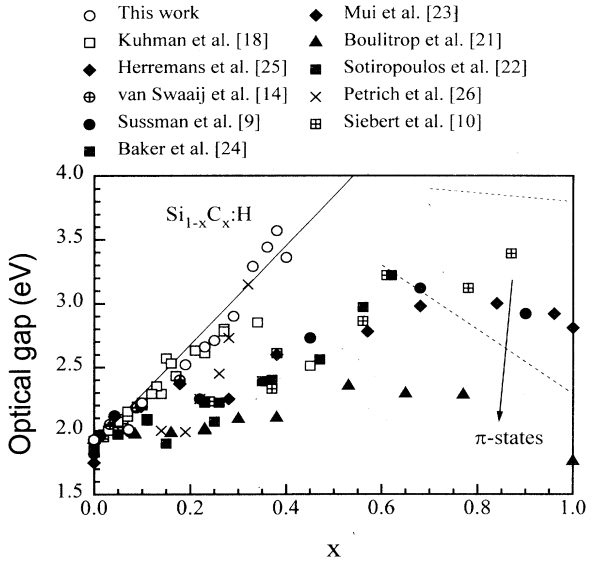


FIG. 1. Optical gap $E_{04}$ as a function of the carbon content from different laboratories. The brackets indicate the corresponding reference numbers The full line represents the result of the tight-binding calculation by Robertson (Ref. 20). The region between the dotted lines in the right corresponds to $\pi$ states.

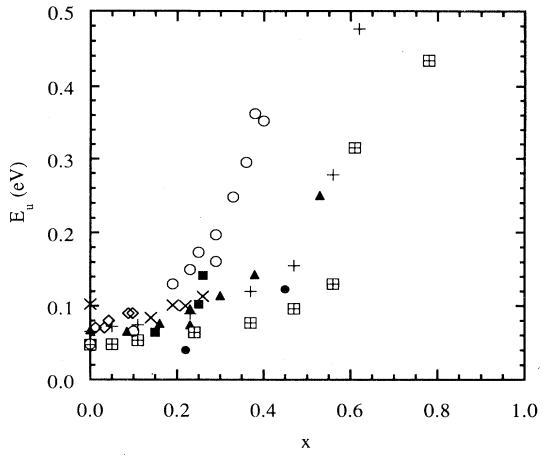


FIG. 2. Measured Urbach parameters $E_u$ as a function of the carbon content from different laboratories. The symbols are the same as in Fig. 1.

### B. Photoluminescence

The normalized PL spectra at 77 K for all samples are represented in Fig. 3. All these spectra were taken with the excitation energy above and very close to $E_{04}$, in or-

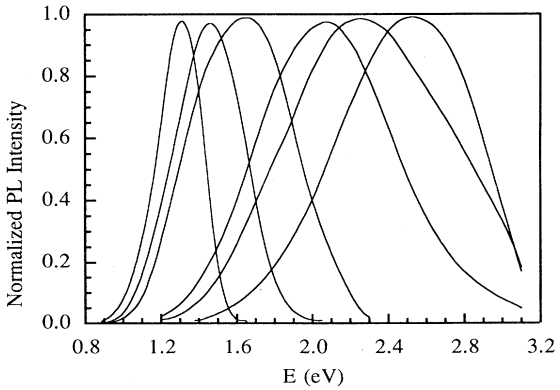


FIG. 3. Some typical normalized PL spectra. The carbon contents $x$ are, from left to right, 0, 0.10, 0.19, 0.24, 0.37, 0.40.

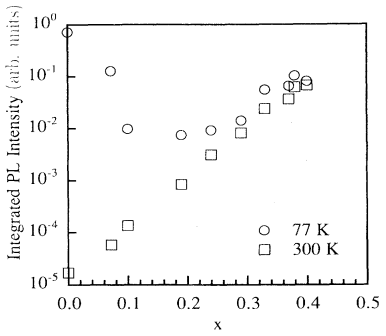


FIG. 4. Integrated PL intensities corrected for the generation rates at 77 and 300 K. Although systematic errors limit the comparison between different samples to an estimated incertitude of 30%, the ratio between low- and room-temperature data for each sample is much better.

der to prevent the PL band narrowing reported for subgap excitation.[7,10]

The integrated PL intensities corrected for the generation rates at 77 K and at room temperature are represented in Fig. 4.

In order to discuss our data, let us review the present models for photoluminescence in *a*-Si:H. As pointed out in the Introduction, there is still not universal agreement concerning the process that determines the photoluminescence band width and position.

### 1. *Low-temperature photoluminescence*

In *a*-Si:H the photoluminescence efficiency $\eta$ is very high at low temperatures[27] ($\eta \sim 0.3$). The PL process is the result of the competition between radiative and nonradiative recombination channels. Radiative recombination occurs by transition between an electron and a hole, each in a localized state in the band tails. The nonradiative process is primarily associated with a defect lying near midgap (like the Shockley-Read process) as is the case of, for example, a dangling bond. Indeed, the PL intensity decreases very strongly when the dangling bond density increases.[5]

For low excitation rates the radiative recombination is germinate. The radiative recombination rate $\tau_r^{-1}$ of an electron and a hole in the band tails is determined by the overlap of the wave functions:[5]

$$\tau_r = \tau_{0r} \exp(2R/R_e) , \tag{5}$$

where $\tau_{0r}$ is the lifetime for completely overlapping electron and hole wave functions, $R$ is the carrier separation, and $R_e$ is the localization length of the electron, assumed to be the less localized carrier. Carrier separation arises from the diffusion of carriers in the extended states during thermalization.

The lifetime $\tau_{0r}$ is derived from Fermi's golden rule:[28]

$$\frac{1}{\tau_{0r}} = \kappa^{1/2} \frac{E_\varphi^3 e^2 |\langle i|x|f\rangle|^2}{3\hbar^4 c^3} , \tag{6}$$

where $\kappa$ is the dielectric constant of the medium, $E_\varphi$ is the energy of the emitted photon, $e$ is the electron charge, $c$ is the speed of light, and $\langle i|x|f\rangle$ is the dipole-matrix element between the initial and final states. For perfectly overlapping localized wave functions the dipole-matrix element can be approximated by[28]

$$|\langle i|x|f\rangle|^2 \sim \frac{(2R_h)^5}{(R_e)^3} , \tag{7}$$

where $R_h$ is the hole localization length. For pure *a*-Si:H, PL decay data are well fitted supposing[29] $\tau_{0r} \sim 10^{-8}$ sec, corresponding to $R_e \sim 1.1$ nm and $R_h \sim 0.3$ nm.

Since at low temperatures the carriers are frozen in the tail states with very low mobility, the nonradiative recombination process is also tunneling limited. Then the non-radiative lifetime $\tau_{nr}$ is also determined by the less localized carrier:

$$\tau_{nr} = \tau_{0nr} \exp(2r/R_e) , \tag{8}$$

where the "attempt-to-escape" frequency $\tau_{0nr}^{-1} = \nu_0 \cong 10^{-12}$ sec corresponds to a typical photon frequency and $r$ is the distance between the electron and the nonradiative center.

A critical distance $R_c$ can be defined[5] such that for a carrier whose distance to a nonradiative recombination center is smaller than $R_c$ the probability of nonradiative recombination is higher than the probability of radiative recombination. From (5) and (8) it follows that

$$R_c = \frac{R_e}{2} \ln(\nu_0 \tau_{0r}) . \tag{9}$$

For *a*-Si:H, with its relatively narrow PL band (when compared with the alloys), $R_c$ can be considered constant within the whole band tails.[5] A good fit to experimental data is obtained for $R_c \sim 12$ nm.

The origin of the photoluminescence bandwidth has been attributed alternatively to an electron-phonon–induced lattice relaxation process (Stokes shift) or as a natural consequence of the existence of band tails due to static disorder. The next sections describe briefly the main predictions of each. To date, there is still no universal agreement about which of them is the most important.

*a. The Stokes-shift model.* In the simplest form of the Stokes-shift process,[30] the photoluminescence peak $E_L$ is shifted due to the relaxation of the lattice configurational energy in the excited state (Stokes shift) by an amount $E_S$. Thus $E_L = E_A - E_S$ where $E_A$ is the peak in the absorption band. In an amorphous semiconductor there is a continuum of possible excited states and the absorption band grows monotonically instead of presenting a peak. Consequently $E_A$ is not a well-defined energy. Since the PL bandwidth depends on the excitation energy below $E_{04}$ but not above it,[7,10] we shall estimate $E_A$ to be equal to $E_{04}$. For excitation above $E_A$, photogenerated carriers rapidly lose energy (thermalize) by phonon emission while jumping between states. This thermalization process may also continue within the localized tail states, since $E_A$ may in fact be different from the mobility edge.

Due to the thermalization process $E_L$ may be shifted by the energy $E_{\rm th}$ lost by the carriers before recombination. This thermalization term should be included for the calculation of $E_L$:

$$E_L = E_{04} - E_S - E_{\rm th} \ . \tag{10}$$

The photoluminescence bandwidth in case of relaxation via a single phonon energy $\Delta E_L^{e\text{-ph}}$ is given by

$$\Delta E_L^{e\text{-ph}} = 2[\ln(2) E_s E_0]^{1/2} \ , \tag{11}$$

where $E_0 = h\nu_0$ is a typical phonon energy. The typical phonon frequency $\nu_0$ is the same as used in Eq. (8).

*b. The static disorder model.* In the static disorder model,[6] the photoluminescence band shape is a result of the steady-state carrier distribution within the assumed exponential band tail density of states available for radiative recombination. After having thermalized rapidly to the band edges, photogenerated carriers start a much slower thermalization within the band tails up to $\tau_r$, corresponding to transitions among states over distances up to $R_c$. Radiative recombination then takes place between states that are the lowest within spheres of radius $R_c$ in each band. For each exponential band tail, the density $P_i$ of such states is

$$P_i(\varepsilon) = N_{0i} \exp(-\varepsilon / E_{\alpha i}) \times \exp[-v_c(\varepsilon) N_{0i} E_{\alpha i} \exp(-\varepsilon / E_{\alpha i})] \ , \tag{12}$$

where $i$ indicates the band (valence or conduction), $N_{0i}$ is the density of states of the band $i$ at the mobility edge, $\varepsilon$ is the energy of the state measured from the mobility edge, $v_c$ is the volume of a sphere of radius $R_c$, and $E_{\lambda i}$ are the characteristic energies of the exponential densities of states. Considering $v_c$ independent of $\varepsilon$, Eq. (12) corresponds to a slightly asymmetric Gaussian-like shape with a maximum at $\varepsilon_{\rm max}$:

$$\varepsilon_{\rm max} = E_{\lambda i} \ln(v_c N_{0i} E_{\lambda_i}) \tag{13}$$

and a width $\Delta\varepsilon_i$ independent of $v_c$:

$$\Delta\varepsilon_i \cong 2.45 E_{\lambda i} \ . \tag{14}$$

The PL spectrum is obtained by the convolution of the density of minima described by Eq. (12) for each band tail. This convolution has to be calculated numerically. The characteristic energies $E_{\lambda i}$ reflect the densities of states available for radiative recombination. The exponential slopes of the band tails $E_{\alpha i}$ have been measured for *a*-Si:H. The slope of the valence band $E_{\alpha V}$ is 2 to 3 times higher than that of the conduction band[31] $E_{\alpha C}$. The parameter $E_{\alpha V}$ is identified with the Urbach parameter $E_u$ obtained from absorption measurements. It is tempting to associate $E_{\lambda i} = E_{\alpha i} = E_u$, and this has been done in previous papers.[6,7,19] However, absorption by localized-to-localized transitions [the inverse of the process described by Eq. (5)] is much less probable than absorption by localized-to-extended transitions due to the wave-function overlap factor. Nevertheless, since the luminescence comes from the convolution of electron and hole localized states distributions, and absorption reflects the superposition of such states, $E_{\alpha i} \leq E_{\lambda i}$. This will be discussed in more detail in Sec. III B 1 c.

Searle and Jackson[7] noted that, because of the difference of characteristic energies, the valence band tail distribution of minima $P_V(\varepsilon)$ is much wider than the corresponding conduction band tail distribution $P_C(\varepsilon)$, and is by itself a good approximation for the photoluminescence spectrum. For any *a*-$Si_{1-x}C_x$:H alloy with $x < 0.5$ the band edges remain siliconlike,[20] with the valence band tail *p*-like and the conduction band tail *s*-like. Since the symmetry of *p*-like states is much more sensitive to disorder than that of *s*-like states, we expect small variations in $E_{\alpha C}$ related with carbon alloying, with most of the disorder effects affecting $E_{\alpha V}$. Thus we shall also make the assumption that the valence band tail dominates the PL band shape, which corresponds to approximate the narrow $P_C(\varepsilon)$ by a delta function.

*c. The a-Si:H like samples ($x < 0.3$): Photoluminescence bandwidth and band shape.* In principle, both the electron-phonon process and static disorder contribute to the photoluminescence bandwidth. The two photoluminescence bands are Gaussian-like near the peak, so that the widths add as

$$(\Delta E_L)^2 = (\Delta E_L^{e\text{-ph}})^2 + (\Delta E_L^{\rm stat})^2 \ . \tag{15}$$

In the Stokes-shift model $(\Delta E_L^{e\text{-ph}})^2$ scales with $E_s$ while in the static disorder model $\Delta E_L^{\rm stat}$ scales with $E_u$. Following Searle and Jackson,[7] we tested the predictions of expressions (6) and (9). If the Stokes-shift process is dominant,

$$(\Delta E_L)^2 = 4\ln(2)(E_{04} - E_L - E_{\rm th}) E_0 + (\Delta E_L^{\rm stat})^2 \ . \tag{16}$$

In Fig. 5 we represent $(\Delta E_L)^2$ against $E_{04} - E_L$, so the

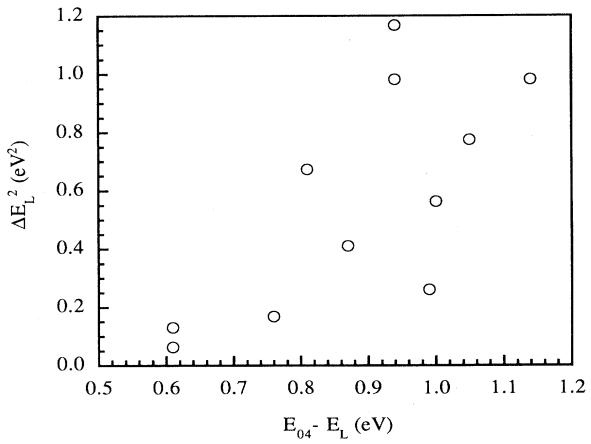


FIG. 5. The squared experimental PL spectrum width vs the PL peak separation from the gap $E_{04} - E_L$. According to the Stokes-shift model, all the data should lie in a single straight line.

zero intercept yields $(\Delta E_L^{\text{stat}})^2 - 4\ln(2)E_{\text{th}}E_0$. The typical phonon energy $E_0$ is obtained from the slope. The experimental points present some scattering. Forcing a straight-line fit, we obtain $E_0 = 0.569 \pm 0.170$ eV. This value is roughly ten times the energy of a typical phonon in *a*-Si:H, which is about 60 meV. Furthermore, even if the disorder term is negligible, the value obtained for $E_{\text{th}}$ is $\sim 0.53$ eV, which corresponds to twice the PL bandwidth. These results are not physically acceptable and indicate that the electron-phonon interaction is not the main reason for the PL bandwidth.

If static disorder is dominant, Eq. (15) can be written as

$$(\Delta E_L)^2 = (2.45\Delta E_u)^2 + (\Delta E_L^{e\text{-ph}})^2 \ . \tag{17}$$

Figure 6 represents $\Delta E_L$ against $E_u$. The straight-line fit is better than in Fig. 5, but the samples with the highest $E_u$ (and highest values of $x$) are below the linear best fit. These samples will be treated in detail in Sec. III B *a b*, and we will not consider them for the moment. The zero intercept is $-0.040 \pm 0.056$ eV, confirming the conclusions of Searle and Jackson[7] that the electron-phonon contribution for the PL width is negligible. In the worst case, assuming $E_{\text{ph}} \sim 60$ meV, it indicates that for *a*-Si:H $E_S = 0.010 \pm 0.019$ eV. This value is comparable to the ones obtained by Searle and Jackson[7] (0.02 eV) and by Schmidt de Magalhães *et al.*[33] (0.036 eV), but much smaller than the 0.5 eV obtained by Street[5] who attributed the PL bandwidth to the electron-phonon interaction only. The validity of the extrapolation of alloy data to pure *a*-Si:H has been questioned[32] in the case of *a*-$SiN_x$:H. The present results, however, were obtained in low-power *a*-$Si_{1-x}C_x$:H, which has an electronic structure[8,17] very similar to that of *a*-Si:H for low $x$ (up to 0.2), carbon being tetrahedrally coordinated. We claim that for our samples the extrapolation to $x = 0$ is justified, and our data provide definitive support for the static disorder model.

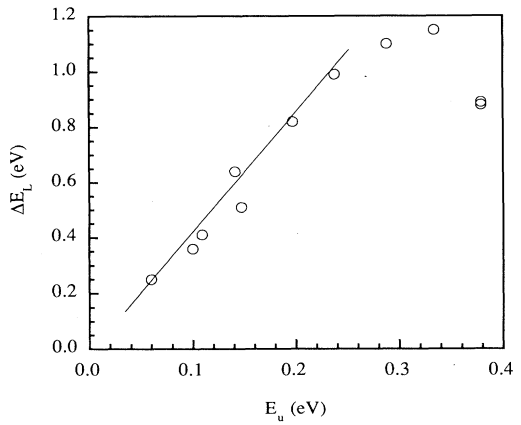


FIG. 6. The PL spectrum width as a function of the Urbach parameter $E_u$. The prediction of the static disorder model of Dunstan *et al.* (Ref. 6) is a straight line with slope 2.45. The slope of the best fit is 3.85 instead, and we attribute the difference to the fact that in *a*-$Si_{1-x}C_x$:H the effective energy parameter of the exponential band tail density of states for luminescence is not quite the Urbach parameter. In the samples with $x > 0.25$ a different radiative recombination mechanism becomes predominant (see text).

The slope of the straight line fit of fig. 6 is $3.85 \pm 0.30$, higher than the 2.45 predicted by Eq. (14). Searle and Jackson[7] found $4.4 \pm 0.2$ for their *a*-$SiN_x$:H. More recently a value of 3.3 can be directly obtained from the results of Magalhães *et al.*[33] for low carbon concentration HP *a*-$Si_{1-x}C_x$:H prepared under hydrogen dilution. Palsule *et al.*[34] found 1.8 for *a*-$Si_{1-x}C_x$:H prepared by rf sputtering. However, the photoluminescence peaks of the latter authors do not follow the variation of the gap, suggesting that their sputtered samples may be inhomogeneous. Searle and Jackson[7] concluded that although the underlying assumptions of the static disorder model are correct, the detailed description of the luminescence process as described above is wrong, and suggested that the disagreement between theory and experiment comes from an oversimplified treatment of the statistics. In particular, they questioned the correctness of considering the critical volume $v_c$ well defined and constant. We investigated the effects of letting $v_c$ vary in Eq. (12), by expanding the function near its maximum. Our conclusion is that up to second order in $\varepsilon/E_\lambda$ (which corresponds to approximating the distribution by a Gaussian) the effect of the variation of $v_c$ over the maximum position is proportional to $\ln(\partial v_c/\partial\varepsilon)$, and its effect over the width is *negligible.* The only way to *increase* the 2.45 coefficient of Eq. (14) is to suppose critical volumes that *increase* with $\varepsilon$, a rather unphysical situation.

The variation of critical volume within the bands is not the cause for the lack of agreement between theory and experiment. However, although the Urbach parameter increases with the disorder, there is no reason to have perfect equality between $E_{\alpha V}$ and $E_{\lambda V}$. As said before, each characteristic energy is related to a different process, the former to absorption and the latter to absorption followed by diffusion, so it is natural to expect them to be proportional rather than equal. To the first order, we can define $\beta = E_\lambda/E_\alpha$. The effect of disorder can be described in terms of parallel and antiparallel potential fluctuations. The former reflects the medium- and long-range variations due to, for instance, average composition fluctuation that exist in any nonstoichiometric alloy. The latter is associated with atomic scale potential fluctuations, as a distorted bond or the precise site of a carbon atom. Absorption is sensitive only to the antiparallel potential fluctuations, while after the thermalization process the carriers can access states that are related to both parallel and antiparallel fluctuations. This will be expressed as a higher effective density of states for recombination than for absorption, resulting in $E_{\lambda V} < E_{\alpha V}$. The coefficient $\beta$ is thus an estimation of the medium-range disorder, and its value is always greater than unity. Since the medium-range disorder is expected to be sensitive to sample preparation parameters, it is not surprising that different laboratories render different values of $\beta$. Our

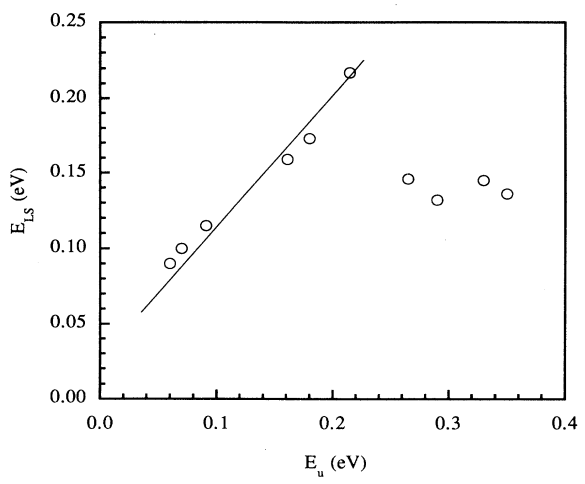


FIG. 7. The low-energy exponential slope of the PL spectrum as a function of the Urbach parameter $E_u$. The straight-line fit corresponds to the prediction of the static disorder model.

data corresponding to very disordered samples yields the highest $\beta$ among the $a$-$Si_{1-x}C_x$:H, but for $a$-$SiN_x$:H it is even higher.[7] Since $\beta$ is close to unity and $E_u$ is easily measurable, equating $E_\lambda$ and $E_u$ is convenient for modeling purposes.

Equation (12) predicts the low-energy side of the photoluminescene band to be exponential with characteristic energy $E_{LS}$ equal to $E_\lambda$. Figure 7 shows $E_{LS}$ vs $E_u$. For $E_u$ smaller than 0.25 eV $E_{LS}$ follows $E_u$. This is in contrast with $a$-$SiN_x$:H for which[7] $E_{LS}$ has no relation with $E_u$. Again this indicates that for low carbon concentration low-power $a$-$Si_{1-x}C_x$:H is more closely akin to pure

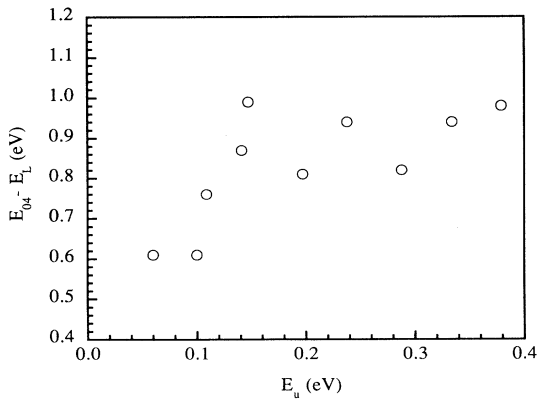


FIG. 8. The PL peak separation from the gap $E_{04}-E_L$ vs the Urbach parameter $E_u$. The data do not correspond to a straight line intercepting the origin as predicted by Dunstan *et al.* (Ref. 6). We attribute this to the decrease of the critical radius $R_c$ as $x$ increases (see text).

$a$-Si:H.

The PL peak position in the static disorder model is essentially the prediction of Eq. (13) for $v_c$ constant, shifted 0.1–0.2 eV due to the convolution with $P_C(\varepsilon')$. Figure 8 shows that indeed there is a weak correlation between $E_{04}-E_L$ and $E_u$. However, the average value of $v_c$ decreases exponentially with the carbon content $x$, following the variation of the density of states at the Fermi level[16] for $x>0.06$. The product $N_0E_u$ is not expected to depend strongly on $x$. The combined effect is that the variation of the logarithmic term compensates the variation of $E_u$ and consequently $E_{04}-E_L$ depends very weakly on $E_u$.

### 2. *Luminescence efficiency and temperature dependence*

*a. The model for good quality a-Si:H.* For pure $a$-Si:H, the temperature dependence of the photoluminescence above 50 K is closely related to the temperature dependence of the carrier mobility.[5] The nonradiative lifetime $\tau_{nr}\sim 10^{-12}$ sec is so much shorter than the radiative lifetime $\tau_r\sim 10^{-3}$ sec that it can be assumed that any carrier trapped in the band tails that is thermally activated to the mobility edge has enough mobility to eventually reach a nonradiative recombination center. Thermal activation to the mobility edge is the most probable event for carriers at states shallower than a demarcation level $E_D(T)$ such that

$$\nu_0\tau_r=\exp[E_D(T)/kT]\ . \tag{18}$$

Supposing that the limiting process is the thermal activation of carriers in the wider band tail, the luminescence efficiency $\eta$ is given by the fraction of carriers deeper than $E_D$:

$$\eta(T)=\eta_0\exp[-E_D(T)/E_u]$$
$$=\eta_0\exp\left[-\frac{kT}{E_u}\ln(\nu_0\tau_r)\right]\ . \tag{19}$$

Since $\ln(\nu_0\tau_r)$ varies very weakly with the temperature, an activated behavior is expected. This simple picture ignores the possibility of carriers hopping directly to the nonradiative recombination centers, since it is negligible in good quality $a$-Si:H in this temperature range. In the alloys, however, with their increased density of states in the gap, $\eta(T)$ shall be reduced due to this process.

*b. Alloys with high carbon concentration ($x>0.3$): High photoluminescence efficiency at room temperature.* The low-temperature luminescence efficiency decreases with carbon alloying, up to approximately $x=0.2$, as shown in Fig. 4. In this carbon concentration range the effect of carbon incorporation in the luminescence efficiency is quite clear. Alloying increases both $E_u$ and the density of silicon dangling bonds that act as fast nonradiative recombination centers. The temperature quenching between 77 and 300 K is reduced mainly due to the increase of $E_u$, as described by Eq. (19).

As the carbon content increases above $x=0.2$, however, the photoluminescence efficiency starts to increase and the temperature quenching decreases, although the densi-

ty of silicon dangling bonds starts to increase more abruptly with the carbon content.[16]

The decrease of the temperature dependence of the luminescence efficiency and increase of its absolute value indicate that not only the radiative recombination rate $\tau_r$ decreases[12,34,35] for these alloys, but also the radiative recombination rate for completely overlapping wave functions $\tau_{0r}$. Indeed, values of $\tau_{0r}$ as low as $\sim 10^{-10}$ sec have been reported[36,37] for different forms of $a$-$Si_{1-x}C_x$:H with low to moderate carbon content. We would like to note, however, that in our wide-gap high-$E_u$ samples the concept of a mobility gap is very ill defined, and that $E_{04}$ that we are using to characterize the gap may correspond to transitions among band tail states. For instance, in the sample with $x=0.4$ the exponential dependence of $\alpha(h\nu)$ continues well above $E_{04}$.

In these alloys with high $E_u$, the density of band tail states is very high, the wave functions are very localized, so that nearest-neighbor hopping[38] is the predominant transition within a band. Nonradiative recombination would be expected to occur if the carrier could reach a deep state. The *only* possibility to explain the high luminescence efficiencies is to assume that, just like in good quality $a$-Si:H at low temperatures, in these samples the carriers recombine radiatively before they can reach the nonradiative centers. We still do not have a complete understanding of the factors leading to the shortening of the radiative lifetimes. One possibility is the onset of a strong Coulomb interaction, leading to a fast excitonlike recombination process analogous to molecular luminescence. Since the electron and the hole are separated by a distance of the order of the interatomic distance, the Coulomb energy can be of the order of hundreds of meV, preventing them from separating and accelerating the recombination process. Thus the photoluminescence bandwidth is reduced in relation to the noninteracting case because the carriers recombine before completely probing their neighborhood. This explains why Eq. (15) is not valid for the samples with high carbon content, for which the PL bandwidth is almost independent of $x$. Indeed, recombination kinetics characteristic of an excitonic process has been observed in high-power $a$-$Si_{1-x}C_x$:H of high luminescence efficiency.[12]

## IV. CONCLUSIONS

We presented PL data in a set of low-power $a$-$Si_{1-x}C_x$:H with $0<x<0.45$. This material has negligible amounts of $sp^2$ carbon hybrids, and consequently higher gaps and higher disorder than conventional high-power $a$-$Si_{1-x}C_x$:H. For low carbon concentrations all the carbon is in the form of methyl, while for higher carbon concentrations carbon starts to have multiple bonds to the network. Under excitation intensities that correspond to germinate recombination, we found two different luminescence regimes, more or less coincident with the two regimes of carbon binding:

(a) For low carbon concentrations ($x<0.25$, $E_{04}<2.7$ eV, $E_u<0.2$ eV), as the carbon content increases the low-temperature PL efficiency is reduced, the PL peak shifts to higher energies and the PL bandwidth increases. The PL band is determined by static disorder, i.e., by the distribution of band tail states for which the probability of radiative recombination is higher than the probability of further thermalization in the band. Throughout the whole range of carbon concentrations (including $x=0$, pure $a$-Si:H) the electron-phonon interaction contribution to the PL bandwidth is negligible when compared to the width induced by disorder. This extends earlier conclusions by Searle and Jackson[7] who studied the $a$-$SiN_x$:H system. Since the low-power $a$-$Si_{1-x}C_x$:H system at low carbon concentration has its electronic structure very similar to $a$-Si:H we claim that the present study provides definite support for the static disorder model even for $a$-Si:H. The value obtained for the Stokes shift is $E_S=0.010\pm0.019$ eV. The simplified state disorder theory of Dunstan and Boulitrop[6] correctly predicts the linear dependence of the PL bandwidth and the low-energy tail of the luminescence spectrum on the Urbach parameter. The detailed dependence of the luminescence bandwidth on the Urbach parameter indicates that for the radiative recombination process the effective disorder is higher than for the optical absorption process, which is reasonable when we consider the different electronic processes involved.

(b) For higher carbon contents ($0.25<x<0.4$, 2.8 eV $<E_{04}<$ 3.5 eV, $E_u>0.2$ eV), the PL efficiency increases while the temperature quenching is reduced. For $x=0.4$ the integrated PL efficiency is only a factor 2 below that of pure $a$-Si:H at 77 K and does not present temperature quenching. The PL bandwidth almost does depend on $x$ for excitation at 3.5 eV. This indicates that the radiative process is very fast in these samples, possibly due to the electron and hole being strongly correlated by the Coulomb interaction. The bandwidth is reduced in relation to the noninteracting case as the diffusion process is interrupted by recombination.

## ACKNOWLEDGMENTS

The authors are indebted to Dr. Georges Lampel and to Dr. John Robertson for a critical reading of the manuscript. One of us (L.R.T.) acknowledges support from the European Union/CNPq under the "Marie Curie" Research Initiative.

*On leave from Instituto de Física "Gleb Wataghin," Universidade Estadual de Campinas, 13081-970 Campinas, SP, Brazil; Electronic address: tessler@ifi.unicamp.br

[1]J. Bullot and M. P. Schmidt, Phys. Status Solidi (B) **143**, 345 (1987).

[2]P. G. LeComber, J. Non-Cryst. Solids **115**, 1 (1989).

[3]Y. Hamakawa, D. Kruangam, T. Toyama, M. Yoshimi, S. Paasche, and H. Okamoto, Optoelectronics **4**, 281 (1989).

[4]R. A. Street, *Hydrogenated Amorphous Silicon* (Cambridge University Press, Cambridge, 1991), p. 295.
[5]R. A. Street, Adv. Phys. **30**, 593 (1981).
[6]F. Boulitrop and D. J. Dunstan, Phys. Rev. B **28**, 5923 (1983); D. J. Dunstan and F. Boulitrop, *ibid.* **30**, 5945 (1984).
[7]T. M. Searle and W. A. Jackson, Philos. Mag. B **60**, 237 (1989).
[8]I. Solomon, M. P. Schmidt, and H. Tran-Quoc, Phys. Rev. B **38**, 9895 (1988).
[9]R. S. Sussmann and R. Ogden, Philos. Mag. B **44**, 137 (1981).
[10]W. Siebert, R. Carius, W. Fuhs, and K. Jahn, Phys. Status Solidi B **140**, 311 (1987).
[11]S. Liedtke, K. Lips, M. Bort, K. Jahn, and W. Fuhs, J. Non-Cryst. Solids **114**, 522 (1989).
[12]V. A. Vasil'ev, A. S. Volkov, E. Musabekov, E. I. Terukov, V. E. Chelnokov, S. V. Chernyshov, and Yu. M. Shernyakov, Fiz. Tekh. Poluprovodn. **24**, 716 (1990) [Sov. Phys. Semicond. **24**, 445 (1990)].
[13]S. V. Chernyshov, E. I. Terukov, V. A. Vassilyev, and A. S. Volkov, J. Non-Cryst. Solids **134**, 218 (1991).
[14]R. A. C. M. M. van Swaaij, A. J. M. Berntsen, W. G. J. H. M. van Sark, H. Herremans, J. Bezemer, and W. F. van der Weg, J. Appl. Phys. **76**, 251 (1994).
[15]M. L. de Oliveira, S. S. Camargo, Jr., and F. L. Freire, J. Appl. Phys. **71**, 1531 (1992).
[16]O. Chauvet, L. Zuppiroli, J. Ardonceau, I. Solomon, Y. C. Wang, and R. F. Davis, Mater. Sci. Forum **83-87**, 1201 (1992).
[17]I. Solomon, M. P. Schmidt, C. Sénémaud, and M. Driss-Khodja, Phys. Rev. B **38**, 13 263 (1988).
[18]D. Kuhmann, S. Grammatica, and F. Jansen, Thin Solid Films **177**, 253 (1989).
[19]I. Solomon and L. R. Tessler, in *Amorphous Silicon Technology—1994,* edited by E. A. Schiff, M. Hack, A. Madan, M. J. Powell, and A. Matsuda, MRS Symposia Proceedings No. 336 (Materials Research Society, Pittsburgh, 1994), p. 505; L. R. Tessler and I. Solomon, *ibid.*, p. 613.
[20]J. Robertson, Philos. Mag. B **66**, 615 (1992).
[21]F. Boulitrop, J. Bullot, M. Gauthier, M. P. Schmidt, and Y. Catherine, Solid State Commun. **54**, 107 (1985).
[22]J. Sotiropoulos and G. Weiser, J. Non-Cryst. Solids **92**, 95 (1987).
[23]K. Mui, D. K. Basa, F. W. Smith, and R. Corderman, Phys. Rev. B **35**, 8089 (1987).
[24]S. H. Baker, W. E. Spear, and R. A. G. Gibson, Philos. Mag. B **62**, 213 (1990).
[25]H. Herremans, W. Grevendonk, R. A. C. M. van Swaaij, W. G. J. H. M. van Sark, A. J. M. Berntsen, W. M. A. Bik, and J. Bezemer, Philos. Mag. B **66**, 787 (1992).
[26]M. A. Petrich, K. K. Gleason, and J. A. Reimer, Phys. Rev. B **36**, 9722 (1987).
[27]W. B. Jackson and R. J. Nemanich, J. Non-Cryst. Solids **59&60**, 353 (1983).
[28]S. Kivelson and C. D. Gelatt, Jr. Phys. Rev. B **26**, 4646 (1982).
[29]C. Tsang and R. A. Street, Phys. Rev. B **19**, 3027 (1979).
[30]R. A. Street, *Hydrogenated Amorphous Silicon* (Ref. 4), p. 279.
[31]T. Tiedje, A. Rose, and J. M. Cebulka, in *Tetrahedrally Bonded Amorphous Semiconductors (Carefree, Arizona),* edited by R. A. Street, D. K. Biegelsen, and J. C. Knights (AIP, New York, 1981), p. 197; R. A. Street, *Hydrogenated Amorphous Silicon* (Ref. 4), p. 81.
[32]R. A. Street, *Hydrogenated Amorphous Silicon* (Ref. 4), p. 303.
[33]C. S. de Magalhães, C. Bittencourt, L. R. Tessler, and F. Alvarez, J. Non-Cryst. Solids **164-166**, 1027 (1993).
[34]C. Palsule, S. Gangopadhyay, D. Cronauer, and B. Schröder, Phys. Rev. B **48**, 10 804 (1993).
[35]B. A. Wilson, P. Hu, J. P. Harbison, and T. M. Jedju, J. Non-Cryst. Solids **59&60**, 341 (1983).
[36]E. Nakazawa, H. Munekata, and H. Kukimoto, Solid State Commun. **45**, 925 (1983).
[37]Y. Matsumoto, H. Kunitomo, S. Shionoya, H. Munekata, and H. Kukimoto, J. Non-Cryst. Solids **59&60**, 345 (1983).
[38]N. F. Mott and E. A. Davis, *Electronic Processes in Non-Crystalline Materials,* 2nd ed. (Clarendon, Oxford, 1979), p. 33.